

# Synthesis of Visible-light Activated Nanoparticles for H<sub>2</sub> Production

Abdulmenan M. Hussein and Rajesh V. Shende

Department of Chemical and Biological Engineering  
South Dakota School of Mines and Technology,  
Rapid City, SD 57701 USA, [Rajesh.Shende@sdsmt.edu](mailto:Rajesh.Shende@sdsmt.edu)

## ABSTRACT

A series of visible light active Cr-doped TiO<sub>2</sub> photocatalyst powder was synthesized by the sol-gel method using non-ionic surfactant as structure directing template. The Cr-doped TiO<sub>2</sub> photocatalysts were characterized for surface area, crystal phase, microstructure, elemental analysis and band gap measurement by nitrogen isotherm, powder X-ray diffraction, X-ray fluorescence and UV-Vis diffuse reflectance spectroscopy, respectively. The results of diffuse reflectance spectra revealed that the absorption in the visible region is significantly improved for Cr-doped TiO<sub>2</sub> photocatalyst. The calculated optical band gap is reduced from 3.2 eV (anatase) to ~1.7 eV. The BET specific surface area (SSA) of Cr-doped TiO<sub>2</sub> has shown higher surface area than its analogue TiO<sub>2</sub>. A progressive increase of BET SSA (fine crystal sizes) and red shift in the band gap absorption are noticed with the increasing chromium contents. The performance of Cr-doped TiO<sub>2</sub> was investigated towards H<sub>2</sub> generation from aqueous-methanol solution under AM1.5 simulated solar light illumination. The hydrogen generation rates were compared with the activity of TiO<sub>2</sub> and ZnO photocatalysts. Only a trace amount of hydrogen were produced using Cr-doped TiO<sub>2</sub> nanopowders under UV or visible light irradiation.

**Keywords:** Cr-dopedTiO<sub>2</sub>, visible light, hydrogen

## 1 BACKGROUND

Currently over 95% of H<sub>2</sub> is derived primarily from fossil fuels (natural gas, oil and coal) by steam reforming [1]. In this process, fossil fuels are consumed and CO<sub>2</sub> is emitted, which contaminates the air and may lead to global warming. A promising alternative to fossil fuels is solar H<sub>2</sub> via non-carbon energy sources with very little environmental impact. As a result, photocatalysis over solar irradiated semiconductor surfaces have received great attention for hydrogen production. Photocatalytic water-splitting using a semiconductor offers a promising way for clean, low-cost and environmentally friendly production of solar H<sub>2</sub>. The key component of the photocatalyst system is the semiconductor, which converts incident photons to electron/hole pairs. The ideal photocatalyst should fulfill several tasks at once such as light absorption, charge

separation and transport, and H<sub>2</sub> or O<sub>2</sub> evolution at its surface, stability in aqueous solution and low cost. The majority of photocatalysts are, however, wide band-gap semiconductors which are active only under UV irradiation, constituting 3-5% solar light spectrum.

TiO<sub>2</sub>, by far, the most thoroughly investigated photocatalyst due to its photoactivity, chemical inertness and low-cost. However, TiO<sub>2</sub> has a large band gap and only activated by UV light. Its catalytic activity for water redox reactions at the surface is poor. Therefore, it is of great interest to extend its optical absorption threshold into visible region without decrease of photocatalytic activity.

A variety of approaches have been adapted to improve photocatalytic activity of TiO<sub>2</sub> and expand its optical absorption into visible region by doping with transition metals and nonmetals [2], narrow band-gap semiconductor coupling [3] and dye sensitization [4]. In this study, we prepared series of mesoporous chromium (Cr<sup>3+</sup>) doped TiO<sub>2</sub> similar to our earlier report [4] using sol-gel synthesis method to understand the effects of transition metal-ion doping on photoactivity and visible light optical response of TiO<sub>2</sub>.

## 2 EXPERIMENTAL

### 2.1 Catalyst Preparation

A series of Cr-doped TiO<sub>2</sub> photocatalysts was prepared by acid stabilized sol-gel method using Pluronic 123 as structure directing agent. Figure 1 depicts the preparation flow scheme by sol-gel method.

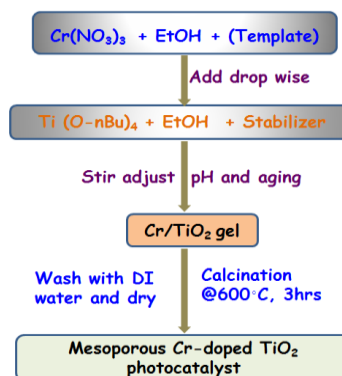


Figure 1: Photocatalyst preparation flow scheme by sol-gel method.

The dried samples were thoroughly washed and calcined in muffle furnace at 550 °C for 3 hours to obtain highly crystalline chromium doped TiO<sub>2</sub> nanopowders. The obtained nanopowders were characterized with X-ray diffraction (XRD), X-ray fluorescence (XRF), nitrogen isotherms and UV-Vis diffuse reflectance spectroscopy (DRS).

## 2.2 Photocatalytic H<sub>2</sub> Generation

Photocatalytic H<sub>2</sub> generation experiments were carried using a semi-batch quartz photocatalytic reactor with 5 mL capacity, equipped with 300 W xenon lamp (Oriel) and AM1.5 filter as a light sources. In a reactor, 2.0 mg of photocatalyst was suspended in 2 mL methanol-water solution (0.4 mL methanol) and sonicated [4, 5]. Prior to irradiation, the reactor suspension was deaerated with ultrapure argon gas for 30 minutes to remove dissolved oxygen. The overhead gaseous products were analyzed for H<sub>2</sub> by a TCD equipped gas chromatograph (Ar as carrier gas). Figure 2 illustrates the processing and illumination steps used for the photocatalytic hydrogen generation studies.

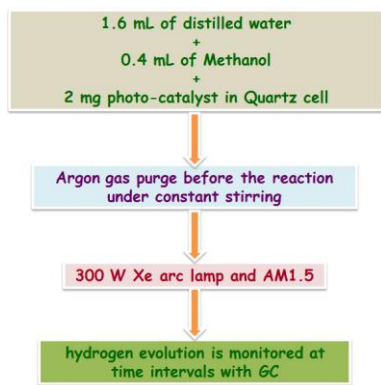


Figure 2: Processing and simulated solar illumination steps used for the photocatalytic hydrogen production.

## 3 RESULTS AND DISCUSSIONS

### 3.1 XRD and XRF Analysis

The XRD patterns of the Cr-doped TiO<sub>2</sub> nanopowders sintered at 550 °C for 5 hours are shown in Figure 3. All the diffraction peaks were indexed to pure anatase phase TiO<sub>2</sub>. No diffraction peaks corresponding to rutile, chromium oxide or mixed chromium titanium oxides were detected. The absence of peaks corresponding to rutile or chromium oxide may be attributed to the thermal stability of anatase phase and to the low atomic concentrations of incorporated Cr<sup>3+</sup>, respectively. The average crystal sizes estimated from Scherrer's equation are in the range of 7-10 nm. Moreover, the surface composition of the obtained nanopowders were further analysed by XRF, which revealed that the chromium content was in good agreement

with the amount of chromium weight percent originally taken for the synthesis.

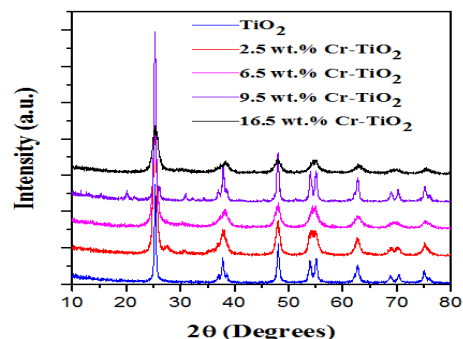


Figure 3: XRD spectra of TiO<sub>2</sub> and Cr-doped TiO<sub>2</sub> nanopowders.

### 3.2 BET Surface Area

The porous properties of Cr-doped TiO<sub>2</sub> powders were examined by N<sub>2</sub> adsorption/desorption isotherms. The shapes of the isotherms were found to be similar regardless of the Cr quantity used (Figure 4). The N<sub>2</sub> isotherm exhibits typical IUPAC type IV pattern (type H2 hysteresis loop), confirming the characteristic of mesoporous structures. A progressive increase in specific surface area was observed with increasing chromium contents. The surface area and pore volume of the samples prepared are summarized in Table 1.

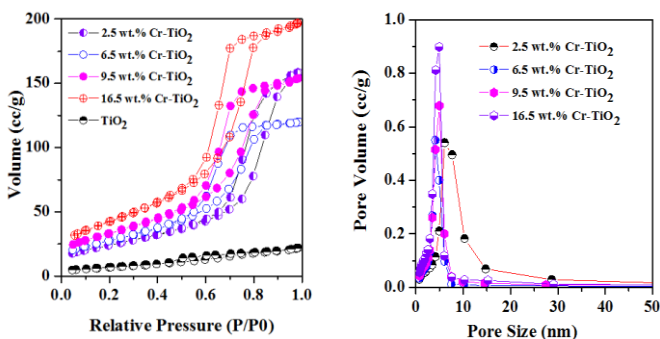


Figure 4: N<sub>2</sub> adsorption/desorption isotherms (left) and pore size distributions of TiO<sub>2</sub> and Cr-doped TiO<sub>2</sub> nanopowders (right).

Table 1: The specific surface area, pore volume and the average pore size, band gap and hydrogen evolution.

| Sample           | Surface area (m <sup>2</sup> /g) | Pore volume (cm <sup>3</sup> /g) | Average pore size (nm) | Band Gap (eV) | H <sub>2</sub> Evolution (mmole/g) |
|------------------|----------------------------------|----------------------------------|------------------------|---------------|------------------------------------|
| ZnO              | 19                               | 0.010                            | 0.81                   | 3.2           | 0.036                              |
| TiO <sub>2</sub> | 58.4                             | 0.010                            | 5.85                   | 3.2           | 0.786                              |
| 2.5 wt. % Cr     | 87.5                             | 0.245                            | 11.2                   | 2.1           | trace                              |
| 6.5 wt. % Cr     | 100.3                            | 0.185                            | 7.40                   | 1.9           | trace                              |
| 9.5 wt. % Cr     | 120.6                            | 0.238                            | 7.90                   | 2.0           | trace                              |
| 16.5 wt. % Cr    | 154.2                            | 0.305                            | 7.90                   | 1.8           | trace                              |

The Cr-modified TiO<sub>2</sub> have higher surface area, smaller crystallite size and greater thermal stability as compared with pure phase TiO<sub>2</sub>, which are important features in photocatalysis.

### 3.3 UV-Vis DRS

The diffuse reflectance spectra of mesoporous TiO<sub>2</sub> and Cr-doped TiO<sub>2</sub> nanopowders in the range of 200–800 nm were examined to determine the optical absorption properties. The results are shown in Figure 5 with the corresponding Kubelka Munk function. All Cr-doped TiO<sub>2</sub> nanomaterials exhibited strong absorption edge beyond pure TiO<sub>2</sub> deep in the visible region of the solar spectrum. The optical energy band gap ( $E_g$ ) determined by applying Kubelka Munk function is presented in Table 1. Upon doping, the optical energy band gap is decreased from 3.2 eV of anatase-TiO<sub>2</sub> to 1.8 eV for 16.5 wt. % Cr-TiO<sub>2</sub>.

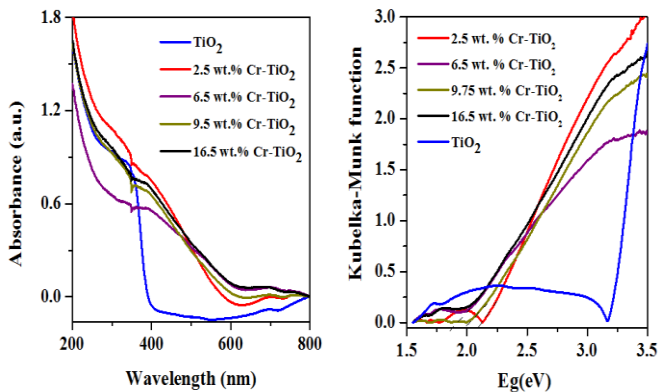


Figure 5: UV–visible spectra of pure TiO<sub>2</sub> and Cr-doped TiO<sub>2</sub> nanopowders (left) and corresponding Kubelka Munk function (right).

### 3.4 Photocatalytic Hydrogen Generation

The photocatalytic performance of the Cr-doped TiO<sub>2</sub> nanopowders were tested by measuring the amount of H<sub>2</sub> generated by direct water-splitting or from methanol-aqueous solution under UV or visible light irradiation. The photocatalytic activities were compared to pure ZnO and TiO<sub>2</sub> nanopowders. However, no significant hydrogen generation (only a trace amount) was observed with Cr-doped TiO<sub>2</sub> nanopowders, showing a clear mismatch between the visible light activation and improving the H<sub>2</sub> generation. This result clearly demonstrates the importance of other parameters, in particular, parameters such as charge carriers mobility, electron/hole lifetime and kinetic barriers than just an appropriate band alignment, crystallinity, high surface area and large pore volume for effective photocatalytic water splitting.

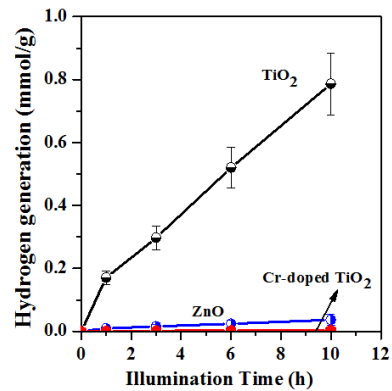


Figure 6: Hydrogen evolution over ZnO, TiO<sub>2</sub> and Cr-doped TiO<sub>2</sub> nanopowders.

### 3.5 Conclusions

To explore the possibility of making new and efficient visible-light activated photocatalysts, we have investigated the effect of chromium doping on electronic and optical properties TiO<sub>2</sub>. The results clearly demonstrated a shift in absorption threshold towards visible region, suggesting the interaction of the Cr atom with TiO<sub>2</sub> and modifying its electronic and optical properties. However, no appreciable photocatalytic activity was observed towards H<sub>2</sub> generation using Cr-doped TiO<sub>2</sub> nanoparticles under UV or visible light irradiation. The poor performances toward photocatalytic hydrogen generation might be attributed to the bulk defects introduced by metal ions doping that could possibly enhance recombination losses.

### 3.6 Acknowledgments

The authors acknowledge the financial and research assistantship support from NSF DGE-0903685 and NSF EPS-0903804.

### 3.7 References

- [1] Kalamaras CM, Efstathiou AM. Hydrogen Production Technologies: Current State and Future Developments. Conference Papers in Energy. 2013;2013:9.
- [2] Zaleska A. Doped-TiO<sub>2</sub>: a review. Recent Patents on Engineering. 2008;2:157-64.
- [3] Gan J, Zhai T, Lu X, Xie S, Mao Y, Tong Y. Facile preparation and photoelectrochemical properties of CdSe/TiO<sub>2</sub> NTAs. Materials Research Bulletin. 2012;47:580-5.
- [4] Hussein AM, Shende RV. Enhanced hydrogen generation using ZrO<sub>2</sub>-modified coupled ZnO/TiO<sub>2</sub> nanocomposites in the absence of noble metal co-catalyst. International Journal of Hydrogen Energy. 2014;39.
- [5] Hussein AM, Mahoney L, Peng R, Kibombo H, Wu C-M, Koodali RT, et al. Mesoporous coupled ZnO/TiO<sub>2</sub> photocatalyst nanocomposites for hydrogen generation. Journal of Renewable and Sustainable Energy. 2013;5:13.